Electronic Supplementary Information

Facile Synthesis of Hierarchical Dendrite-Like Structure Iron Layered Double Hydroxides Nanohybrids for Effective Arsenic Removal

Na Tian,[a] Xike Tian,[a] Xiangwen Liu,[a] Zhaoxin Zhou,[a] Chao Yang,[a] Longlong Ma,[a] Chen Tian,[a] Yong Li[a] and Yanxin Wang*[b]*

[a] Faculty of Materials Science and Chemistry, China University of Geosciences, Wuhan 430074, P. R. China.

[b] School of Environmental Studies, China University of Geosciences, Wuhan 430074, P. R. China.

*Corresponding auther E-mail: xktian@cug.edu.cn; yx.wang@cug.edu.cn. Fax: +86 027 67884574; Tel: +86 027 67884574.

Detailed experimental section

Synthesis of Fe-LDH/SEPs

In a typical procedure, 0.267 M $FeSO_4 \cdot 7H_2O$ and 0.133 M $Fe_2(SO_4)_3 \cdot 5H_2O$ salts were dissolved in deionized water followed by the addition of 1 g SEPs were purchased from Sigma under vigorous magnetic stirring at room temperature for 48 hours. The concentration of total Fe was 0.4 M and $n(Fe^{III})/n(Fe_{total})$ fixed at 1/3. Few Na_2HPO_4 (2×10^{-2} M) was dissolved in the above mixture, then the resulting solution and the basic solution containing 0.47 M Na_2CO_3 and 1 M NaOH were simultaneously mixed and stirred another hour. Finally, the as-prepared products were obtained by filtering and rinsing with deionized water and ethanol and the resulting products were stored in a glass flask sheltered from the air. For the pure Fe-LDHs sample, the synthetic procedure was similar to the above method without SEPs.

Arsenic adsorption

Arsenic trioxide (As_2O_3) and sodium arsenate ($Na_3AsO_4 \cdot 12H_2O$) was used as the arsenic source of As(III) and As(V), respectively. A given amount of Fe-LDH/SEPs were added into a solution with arsenic. The pH values were adjusted with HCl or NaOH solution, and all of the pH measurements were carried out using a pH meter (PXSJ-226, Shanghai Leici Instrument Factory, China).The concentration of the arsenic in the solution was determined by hydride generation atom fluorescence spectrometry(AFS-230E, China) immediately after the separation of the formed solid precipitate from the solution. The quantity of toxic ions adsorbed by per unit mass of the sample, q_e (mg g^{-1}), is calculated using the following equation:

$$q_e=(C_i-C_e)V/M$$

in which C_i is the initial concentration of ions (mg L^{-1}), C_e is the equilibrium concentration of the ions (mg L^{-1}), M is the mass of the sample (g), and V is the volume of the solution (L).

Batch adsorption of As(III) and As(V) was carried out at 298 K with an adsorbent loading of 0.1 g L^{-1}, and all experiments were run at pH 7.0. Typically, the adsorption isotherms were studied at variable initial As(III) concentrations (0.1-50 mg L^{-1}), followed by shaking for 24 h to achieve equilibrium. The kinetic studies were conducted at different intervals in 5 mg L^{-1} of arsenic solution.

Characterization

X-ray powder diffraction patterns (XRD) of the products were obtained on a Bruker D8 Advance diffractometer equipped with graphite monochromatized Cu Kα radiation (λ = 1.5406 Å). Transmission

electron microscopy (TEM) photomicrographs were taken on a Philips CM12 TEM/STEM microscope at an accelerating voltage of 120 kV and a high-resolution transmission electron microscope (HRTEM, JEM-2010FEF) at an accelerating voltage of 200 kV. The field emission scanning electron microscopy (FE-SEM) images were taken on a Hitachi SU8010 SEM. The BET tests were determined via a Micromeritics ASAP-2000 nitrogen adsorption apparatus. The FT-IR spectra were collected with an EQUNOX 55 instrument by diffuse reflectance scanning disc technique from 4000 to 400 cm^{-1} at room temperature. X-ray photoelectron spectroscopy (XPS) was obtained with a MULTILAB2000 electron spectrometer from VG Scientific using 300 W Al Kα radiation. The final concentrations of arsenic were detected by hydride generation atom fluorescence spectrometry (AFS). All samples were dried before characterization by an oven to remove the adsorbed water.

Experimental data
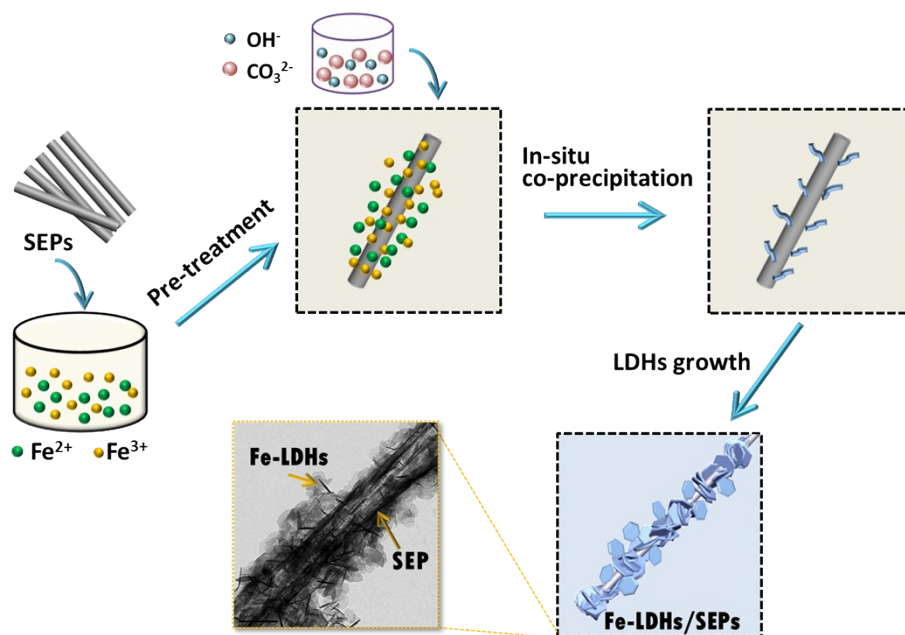
Scheme S1 Schematic illustration for the synthesis of hierarchical dendrite-like Fe-LDH/SEPs.
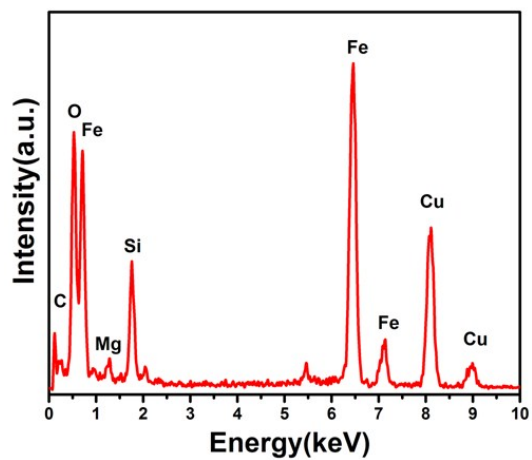

Fig. S1 The energy dispersive X-ray (EDX) of hierarchical dendrite-like Fe-LDH/SEPs.
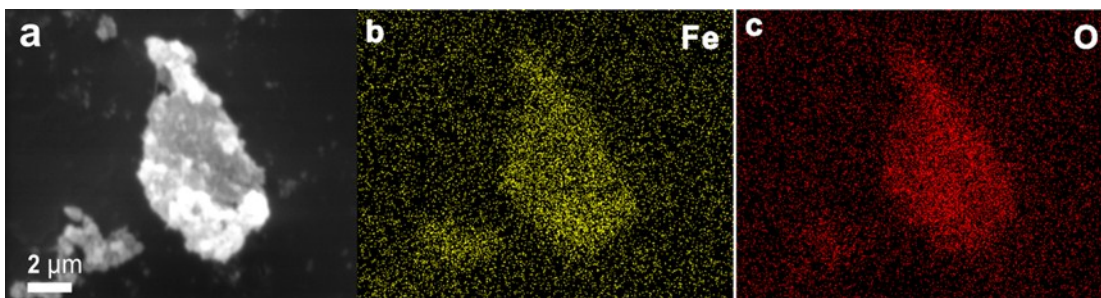
Fig. S2 SEM images (a) of the Fe-LDH/SEPs and corresponding elemental mappings of iron (b) and oxygen (c), suggesting the homogeneous dispersion of Fe and O in these Fe-LDH/SEPs.
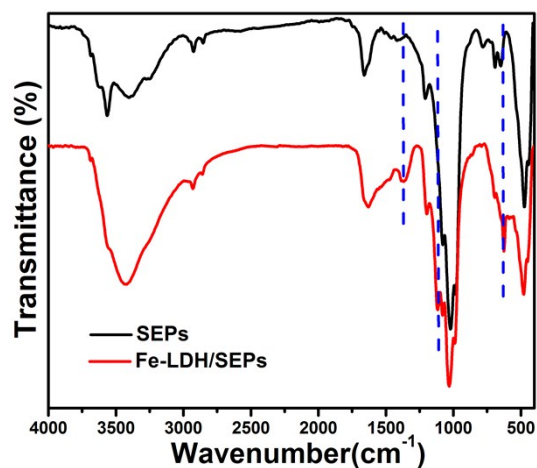

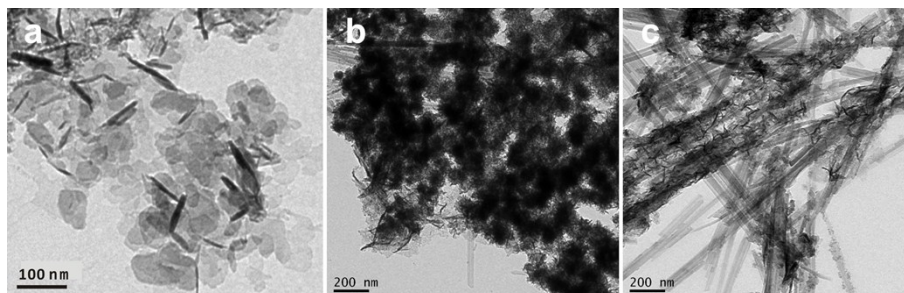**Fig. S3** FT-IR spectra of the pristine SEPs and Fe-LDH/SEPs.

Fig. S4 TEM images of samples synthesized (a) without addition of SEPs, (b) with mass halving of SEPs and (c) with mass doubling of SEPs.
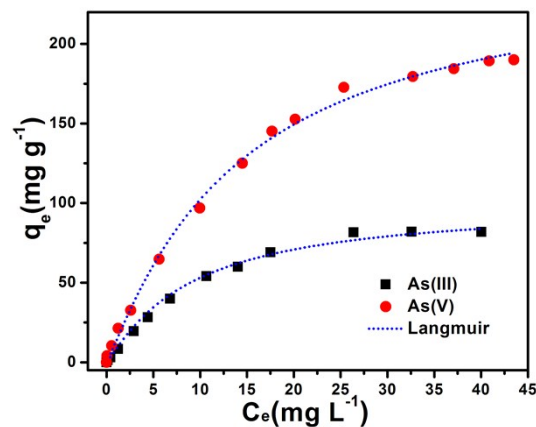
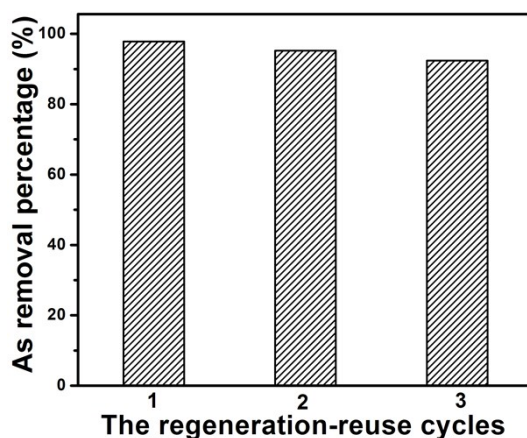Fig. S5 Adsorption isotherms of As(III) and As(V) on pure Fe-LDHs at 298 K.

Fig. S6 The re-adsorption ability of Fe-LDH/SEPs after separation followed by regeneration in real groundwater. Initial arsenic concentration = 465 μg L^{-1}; adsorbent dose = 0.1 g L^{-1}; shaking time = 10 h; pH = 7.0 ± 0.1, and temperature = 25 ± 1 ℃. The used adsorbent was regenerated in a 0.01 M NaOH.
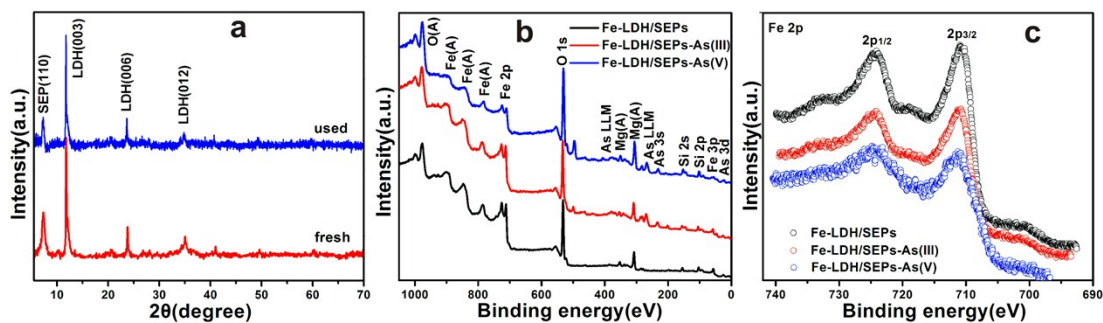

Fig. S7 PXRD patterns (a), XPS survey spectra (b) and the deconvoluted Fe 2p spectra (c) of Fe-LDH/SEPs before and after arsenic adsorption.
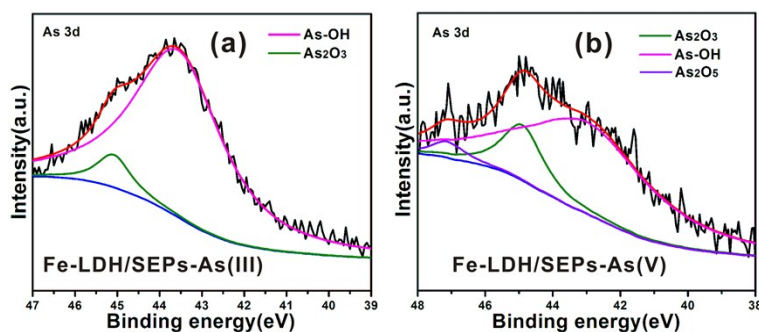
Fig. S8 The deconvoluted As 3d spectra of As(III)-loaded Fe-LDH/SEPs (a) and As(V)-loaded Fe-LDH/SEPs (b).
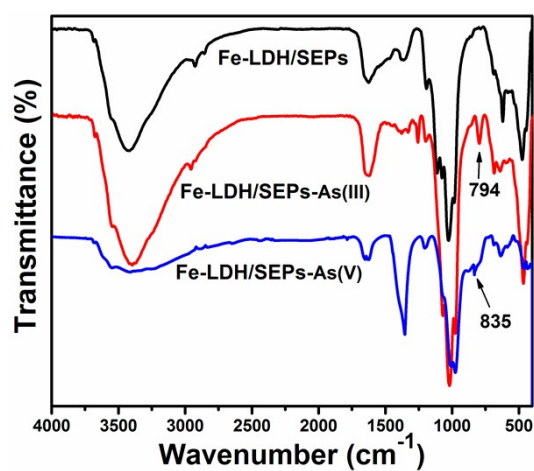
Fig. S9 FT-IR spectra of Fe-LDH/SEPs before and after arsenic adsorption.

Table S1 The calculated Langmuir and Freundlich isotherm parameters for arsenic adsorption on Fe-LDH/SEPs.

Samples	Langmuir isotherm			Freundlich isotherm		
	q_m (mg g^{-1})	K_L (L mg^{-1})	R^2	K_F (mg g^{-1}) (L^3 mg^{-1})$^{-1/n}$	n	R^2
As(III)	135.5	0.1605	0.9891	14.55	1.426	0.9576
As(V)	295.9	0.03383	0.9825	22.62	1.549	0.9494

Table S2 The calculated kinetic parameters for arsenic adsorption on Fe-LDH/SEPs.

Samples	$q_{e,exp}$	Pseudo-first order			Pseudo-second order		
	(mg g^{-1})	k_1 (min^{-1})	$q_{e,cal}$ (mg g^{-1})	R^2	k_2 (g mg^{-1} min^{-1})	$q_{e,cal}$ (mg g^{-1})	R^2
As(III)	27.46	1.12×10^{-2}	15.56	0.9205	1.710×10^{-2}	28.59	0.9985
As(V)	38.01	3.23×10^{-2}	23.92	0.8903	1.771×10^{-2}	37.89	0.9954

Table S3 Comparison of arsenic adsorption capacities.

Adsorbents	Concentration(mg L^{-1})	q_{max}(mg g^{-1}) As(III)	As(V)	Reference
γ-Fe$_2$O$_3$@Carbon	0-18	29.4	17.9	1
Graphene-CNT-γ-Fe$_2$O$_3$	0-10	6.4	/	2
Fe$_3$O$_4$-RGO	3-7	13.1	5.83	3
Iron oxide/CNTs	0-12	8.13	9.74	4
Cellulose@Fe$_2$O$_3$	0-30	23.16	32.11	5
Fe$_2$O$_3$ nanomaterial	0-100	1.25	4.6	6
Fe$_3$O$_4$ nanomaterial	0-100	8.2	6.71	6
Fe-LDH/SEPs	0-50	109.42	262.27	This study

Table S4 Composition of real groundwater in Jianghan Plain, P. R. China.

Composition	Concentration (μg L^{-1})
Chromium	73.14
Nickel	23.11
Copper	5.36
Plumbum	4.32
Arsenic	456
TOC (Total organic carbon)	3013.2
UV$_{254}$	0.05

Table S5 O1s of Fe-LDH/SEPs and As-loaded Fe-LDH/SEPs.

Samples	O-H, 531.5eV	O-Fe, 529.8eV	O-Si, 532.3eV	O-As, 531.0eV
Fe-LDH/SEPs	53.99%	29.04%	16.97%	0
Fe-LDH/SEPs-As(III)	38.34%	38.44%	16.84%	6.38%
Fe-LDH/SEPs-As(V)	0	74.32%	17.44%	8.24%

Reference

1 Z. X. Wu, W. Li, P. A. Webley and D. Y. Zhao, *Adv. Mater.,* 2012, **24**, 485.

2 S. Vadahanambi, S. H. Lee, W. J. Kim and I. K. Oh, *Environ. Sci. Technol.* 2013, **47**, 10510.

3 V. Chandra, J. Park, Y. Chun, J. W. Lee, I. C. Hwang and K. S. Kim, *ACS Nano,* 2010, **4**, 3979.

4 J. Ma, Z. L. Zhu, B. Chen, M. X. Yang, H. M. Zhou, C. Li, F. Yu and J. H. Chen, *J. Mater. Chem. A,* 2013, **1**, 4662.

5 X. L. Yu, S. R. Tong, M. F. Ge, J. C. Zuo, C. Y. Cao and W. G. Song, *J. Mater. Chem. A,* 2013, **1**, 959.

6 S. Luther, N. Borgfeld, J. Kim and J. G. Parsons, *Microchem. J.*, 2012, **101**, 30.